

# APPLICATION OF THE DICHROMATIC REFLECTION MODEL TO WOOD<sup>1</sup>

*Alberto G. Maristany*

Senior Faculty Research Assistant  
Department of Forest Products

*Patricia K. Lebow<sup>2</sup>*

Graduate Student  
Department of Statistics

and

*Charles C. Brunner*

Associate Professor

Department of Forest Products  
Oregon State University  
Corvallis, OR 97331-7402

(Received November 1992)

## ABSTRACT

The applicability of the dichromatic reflection model to describe wood-light interactions in Douglas-fir veneer was investigated. Spectral reflectance measurements taken with illumination along and across the fibers were analyzed by the methodology proposed by Lee et al. (1990). Differences between observed and predicted spectral reflectances were small overall, and increased towards the blue end of the spectrum. Transmission through cell walls, interreflection between cell walls, and an optically active interface are possible explanations for these differences. Average reflectances were higher when samples were illuminated across the directions of the fibers. Rotary-peeled veneer, however, presents surface irregularities where the wood fibers have been pulled away from the surface of the material and where the along-fiber brightness is higher than its corresponding across-fiber measurement.

*Keywords:* Computer vision, color vision, reflection model, spectral reflectance, Douglas-fir veneer, wood surface.

## INTRODUCTION

Computer-automated manufacturing holds great promise for improving the production efficiency and quality of virtually all wood-based products. To reach its full potential,

however, computer vision systems that reliably and economically locate and classify defects on wood surfaces are required. Color information plays a significant role in such systems, as demonstrated by its importance in identifying defects in veneer (Brunner et al. 1992; Butler et al. 1989) and hardwood lumber (Connors et al. 1985). Unfortunately, past computer vision research has largely ignored the specific physical processes that determine color. As a result, color-segmentation algorithms have typically been based solely on statistical methods and heuristic rules (Shafer and Kanade 1987). During the last decade, computer vision has increasingly incorporated

---

<sup>1</sup> This research was partially funded by a special grant from the United States Department of Agriculture as well as by the U.S.D.A. Cooperative State Research Service under Agreement No. 87-FSTY-9-0277. This is paper 2878 of the Forest Research Laboratory, Oregon State University, Corvallis, OR 97331.

<sup>2</sup> Present address: Mathematical Statistician, USDA Forest Service, Forest Products Laboratory, One Gifford Pinchot Drive, Madison, WI 57305.

physical knowledge of surface reflection, illuminant color, and sensor characteristics in developing algorithms (Kanade and Ikeuchi 1991). Collectively, these approaches have been termed "physics-based" vision or "physical modeling in computer vision" (Kanade and Ikeuchi 1991). This new computer vision paradigm has the potential to substantially improve the performance of computer vision systems.

Central to physics-based algorithms are the selection and use of a light-reflection model. This selection involves trade-offs. As Healey (1989) states, "If one desires the most accurate available model, then light-matter interaction can be described in terms of the interaction of photons with atoms or molecules. It would, however, be a formidable task to derive computer vision algorithms from a physical model at such a low level. In computer vision, then, it is often necessary to sacrifice some degree of physical accuracy in order to obtain a model that is useful." One practical model is the dichromatic reflection model (DRM), which was proposed by Shafer (1985) to describe light reflectance from optically nonhomogeneous, opaque, dielectric materials such as plastics or paint. This model is computationally efficient, and has already been integrated into a number of segmentation algorithms (Gershon et al. 1987; Bajcsy et al. 1990; Healey 1990; Klinker et al. 1990; Tominaga 1991; Baribeau et al. 1992; Novak 1992). Healey (1989) has demonstrated that the DRM results closely agree with those of a more detailed reflectance model, the Kubelka-Munk model for predicting the reflectance and opacity of colorant layers (Judd and Wyszecki 1975).

Light striking the surface of dielectric materials is partially reflected at the interface between the surrounding medium and the material (Fig. 1). This reflection is referred to as surface, interface, or Fresnel reflection. On perfectly smooth materials, surface reflection occurs in only one direction, that of perfect-mirror or perfect-specular reflection. Textured surfaces involve more complex patterns of reflection with surface-reflected light scattered in

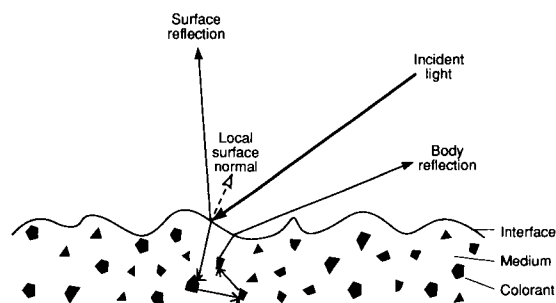


FIG. 1. Light reflection from an opaque nonuniform dielectric material (adapted from Klinker 1988).

many directions (including the perfect-specular direction). The amount of light reflected at the interface depends on the surface smoothness, the incidence angle, and the refraction indices of the material and the surrounding medium (Fresnel's laws). The interface-reflected light is responsible for the glossy appearance of many objects, and is assumed to possess a spectral composition similar to the light source. This is because the refraction indices of most materials are virtually constant across the visible wavelengths (Shafer 1985; Lee 1986; Lee et al. 1990).

Light that is not reflected at the surface penetrates into the subsurface, where it is selectively absorbed and reflected by pigment particles embedded in the material's transparent medium. Any light that emerges from the material's body is highly scattered, and is referred to as body, diffuse, or Lambertian reflection (Fig. 1). This body reflection is responsible for a dielectric material's color (Shafer 1985; Hunter and Harrold 1987). According to the DRM, the spectral distribution of the reflected light from each reflection component is independent of viewing geometry. The model, as originally described, assumes that the material is optically isotropic with respect to rotation around the normal, that the surface is optically inactive (has no pigment protrusions, fluorescence, or thin-film properties), and that pigments are randomly distributed in the material body.

Recent investigations indicated that the DRM adequately describes the interaction of

light with a wide variety of dielectric materials such as plastics, paints, vinyls, tiles, fruits, and leaves (Lee et al. 1990; Tominaga 1991). According to these studies, paper does not follow the DRM. The studies differ, however, with regard to the optical behavior of cloth. One study (Lee et al. 1990) showed that the DRM was appropriate for cloth, whereas the other (Tominaga 1991) indicated that the DRM was not, and suggested that this was because cloth fibers scatter and absorb light in a complicated manner. Both studies found that the DRM was applicable to wood, another fibrous material (Lee et al. 1990; Tominaga 1991). Lee et al. (1990) utilized a single unidentified wood specimen coated with clear vegetable-based oil (Lee 1991), whereas Tominaga (1991) utilized several specimens of uncoated, Japanese cypress lumber (Tominaga 1992).

The objective of this study was to evaluate how the optical properties of rotary-cut Douglas-fir (*Pseudotsuga menziesii* [Mirb.] Franco) veneer affect the applicability of the DRM. The reflectance factors of various surface features in Douglas-fir veneer were measured under different viewing conditions and were tested by the methodology proposed by Lee et al. (1990). The results from this study can be applied to the computer analysis of this type of material.

#### OPTICAL PROPERTIES OF WOOD

In optically isotropic materials, surface orientation does not affect the amount or quality of light reflected at a given illumination and viewing geometry. Wood is an optically anisotropic material composed of different cell types that are typically a hundred times longer than they are wide and are oriented in all three dimensions. Thus, light reflection varies with the angle between the direction of fiber orientation and the incident light rays. Previous studies indicate that, when viewed along the normal and with fibers parallel to the wood-sample surface, brightness is greater with illumination across the fiber direction than along it (Gray 1961; Matthews 1987). This is because a larger

cell-wall area is exposed in the across-fiber direction.

Wood-surface reflection is further complicated by the presence of growth features. In many species, cell characteristics change during the growing season, and this results in distinct growth rings. In particular, in the latter part of the growing season such conifers as Douglas-fir produce latewood cells, which have smaller lumens and thicker walls than do earlywood cells. These cells also differ in light-reflection properties. Another growth feature, the knot, represents transversal sections of branches that were surrounded by the growth of the tree. Knot fibers are aligned with the normal of the wood sample's surface. Incorporation of living branches into the main stem of a tree results in knots that do not become loose upon drying (intergrown or tight knots), whereas incorporation of dead branches produces knots that may fall out as drying takes place (encased or loose knots) (Haygreen and Bowyer 1982).

Wood-light interaction can be affected also by the mechanical process used to create its surface. For example, broken fiber bundles produce greater peaks and valleys in earlywood surfaces of rotary-peeled veneer than in latewood surfaces (Fig. 2). Together, changes in fiber orientation and cell structure cause variations in reflection across cut-wood surfaces, including those that have been planed smooth. These conditions suggest that applying the DRM to wood surfaces may be difficult.

Another complication involves optically active surfaces. Lignin is a mildly fluorescent compound that composes from one-fourth to one-third of the cell-wall material in wood (Haygreen and Bowyer 1982). Resin, produced by some conifers, including Douglas-fir, is even more fluorescent (Haygreen and Bowyer 1982). Although resin is generally confined to small intercellular resin canals, it can at times saturate large areas of wood as a pitch pocket or pitch streak. Bark also fluoresces. In many wood species, pigments produced as the tree ages and older parenchyma cells die might protrude at the material's surface. These pigments

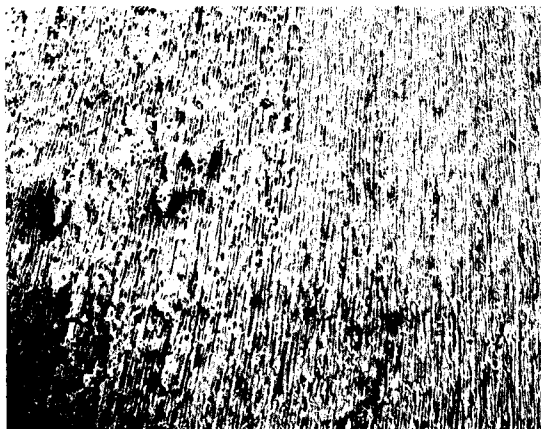


FIG. 2. Scanning electron micrograph of earlywood (left) and latewood (right) in Douglas-fir veneer sapwood ( $\times 15$ ).

produce highly colored extractives that migrate into the lumens of the adjacent wood cells and create the heartwood zone.

Wood-light interactions can be affected by the application of a clear varnish or oil finish, e.g., that used in Lee et al.'s investigation (1990). This produces a smoother surface, which reflects a greater proportion of light in the direction of perfect-mirror reflection and, therefore, mixes lesser amounts of interface-reflected light with body reflection (Overheim and Wagner 1982). The result is a more saturated, richly colored wood surface, which would appear more likely to conform to the DRM than does that of uncoated wood.

The large measurement areas of previous studies (Lee et al. 1990; Tominaga 1991) minimized the influence of textural elements. Researchers studying the applicability of computer vision for inspection of wood surfaces have used spatial resolutions ranging from 15 to 64 pixels per inch (Connors et al. 1983; Forrer et al. 1988, 1989; Butler et al. 1989; Koivo and Kim 1989; Sobey and Semple 1989; Brunner et al. 1992), which correspond to pixel sizes from 1.7 mm to 0.4 mm. The color of pixels representing small wood surface regions can be greatly affected, even with diffuse illumination, by changes in fiber orientation, surface geometry, and texture.

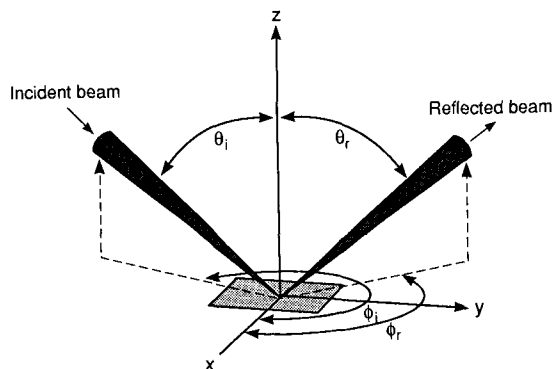


FIG. 3. Geometry of reflectance (redrawn from Nicodemus et al. 1977).

#### REFLECTANCE TERMINOLOGY

At any given wavelength,  $\lambda$ , the light reflected from a point on a nonuniform, opaque, dielectric object,  $f_r$ , can be modeled as the sum of the light reflected at the material surface,  $f_s$ , and the light reflected from the material body,  $f_b$  (Shafer 1985; Hunter and Harrold 1987; Healey 1989). In terms of the spectral bidirectional reflectance distribution functions (Nicodemus et al. 1977), this may be described as

$$f_r(\theta_i, \phi_i; \theta_r, \phi_r; \lambda) = f_s(\theta_i, \phi_i; \theta_r, \phi_r; \lambda) + f_b(\theta_i, \phi_i; \theta_r, \phi_r; \lambda) \quad (1)$$

According to the reflection geometry (Fig. 3), the angles of the illumination direction are represented by  $(\theta_i, \phi_i)$ , and the angles of the viewing or reflected direction are represented by  $(\theta_r, \phi_r)$ . Notation can be simplified for isotropic materials, because reflectance depends only on  $\theta_i$  and  $\theta_r$  (Horn 1986).

The DRM also describes light reflection from a dielectric object as the sum of surface and body reflection,

$$f_r(\theta_i, \phi_i; \theta_r, \phi_r; \lambda) = f_s(\theta_i, \phi_i; \theta_r, \phi_r)C_s(\lambda) + f_b(\theta_i, \phi_i; \theta_r, \phi_r)C_b(\lambda) \quad (2)$$

In this model the color at each image point is the sum of highlight color ( $C_s$ , surface or interface reflection) and object color ( $C_b$ , body or diffuse reflection). The magnitudes (relative

intensities) of these color components, given by the bidirectional reflectance distribution functions  $f_s$  and  $f_b$ , respectively, vary from point to point. The color of the surface and body reflection, however, does not vary across the surface of a single, uniformly colored object.

Following Lee et al. (1990), if a single light source is used and the amount of radiant flux reflected from the surface of interest is compared to that reflected from an ideal, perfectly diffuse, standard surface, then the DRM of Eq. (2) can be expressed in terms of spectral reflectance factors. Suppose the spectral reflectance factors,  $\rho$  at a specific location on an object are measured with respect to two scene geometries, defined by  $\Theta_1 = (\theta_{i_1}, \phi_{i_1}; \theta_{r_1}, \phi_{r_1})$  and  $\Theta_2 = (\theta_{i_2}, \phi_{i_2}; \theta_{r_2}, \phi_{r_2})$ , then they can be described mathematically as

$$\rho(\Theta_1, \lambda) = \rho_s(\Theta_1)C_s(\lambda) + \rho_b(\Theta_1)C_b(\lambda) \quad (3)$$

and

$$\rho(\Theta_2, \lambda) = \rho_s(\Theta_2)C_s(\lambda) + \rho_b(\Theta_2)C_b(\lambda) \quad (4)$$

Solving Eq. (4) for  $C_b(\lambda)$  and substituting into Eq. (3),

$$\rho(\Theta_1, \lambda) = \left[ \rho_s(\Theta_1) - \frac{\rho_b(\Theta_1)}{\rho_b(\Theta_2)} \rho_s(\Theta_2) \right] C_s(\lambda) + \frac{\rho_b(\Theta_1)}{\rho_b(\Theta_2)} \rho(\Theta_2, \lambda). \quad (5)$$

This can be simplified notationally as

$$\rho(\Theta_1, \lambda) = a + m\rho(\Theta_2, \lambda), \quad (6)$$

where  $m$  represents the ratio of intensities from the two scene geometries and  $a$  represents the change in reflectance attributed to the specular properties of the object. Surface reflection,  $C_s(\lambda)$ , is assumed to have the same composition as incident light (Lee et al. 1990), i.e., is constant across the spectrum. Thus,  $a$  does not depend on wavelength.

If  $\rho(\Theta_1, \lambda)$  and  $\rho(\Theta_2, \lambda)$  are obtained for several wavelengths under the two geometric conditions,  $\Theta_1$  and  $\Theta_2$ , then simple linear regression (via least squares) can be used to obtain

estimates of the parameters  $a$  and  $m$ . The vector of responses  $[\rho(\Theta, \lambda_1), \rho(\Theta, \lambda_2), \dots, \rho(\Theta, \lambda_n)]$  plotted against wavelength is referred to as a spectral reflectance factor curve. The appropriateness of the DRM for explaining light reflectance can then be evaluated by a goodness-of-fit measure such as  $R^2$ , the coefficient of determination.

#### EXPERIMENTS

The spectral reflectance factors of seven types of Douglas-fir veneer surface features, including clear wood (earlywood in sapwood), loose knots, tight knots, pitch pockets, pitch streaks, blue stain, and bark, were measured. Five specimens were obtained for each type. Measurements were made in both fiber directions at two different locations on each specimen; this yielded four spectral reflectance curves per specimen, and twenty per feature.

Reflectance curves from the veneer specimens were obtained with a standard 45/0 geometry, in which each sample was illuminated with an incandescent light source at a 45° angle to the surface normal. Measurements were made at the normal. Because of the anisotropic properties of wood, two measurements, one along the fibers and the other across them, were taken. This is equivalent to changing the angle  $\phi_i$  by 90° (Fig. 3), and was accomplished by rotating a single spot on the wood specimen 90° underneath the spectroradiometer receptor.

All wood measurements were preceded by a reference measurement from a Labsphere Spectralon® diffuse reflectance standard. The spectral reflectance factor for each wavelength was obtained by dividing wood energy measurements by reference energy measurements at each wavelength. Measurements were taken every nanometer from 400 to 800 nanometers with a LI-COR 1800 spectroradiometer connected to a UV quartz microscope receptor by a quartz fiber-optic light-guide. The spectroradiometer collected radiant energy from a circular area 0.9 mm in diameter.











